



Published in final edited form as:

Metabolism. 2019 October ; 99: 57–66. doi:10.1016/j.metabol.2019.153946.

Epithelial sodium channels in endothelial cells mediate diet-induced endothelium stiffness and impaired vascular relaxation in obese female mice

James R. Sowers^{1,2,3,4}, Javad Habibi^{1,2}, Annayya R. Aroor^{1,2}, Yan Yang³, Guido Lastra^{1,2}, Michael A. Hill^{3,4}, Adam Whaley-Connell^{1,2,5}, Frederic Jaisser⁶, Guanghong Jia^{1,2,3,5,*}

¹Diabetes and Cardiovascular Center, University of Missouri School of Medicine, Columbia, MO, 65212, USA

²Research Service, Harry S Truman Memorial Veterans Hospital, Research Service, 800 Hospital Dr, Columbia, MO, 65201, USA

³Dalton Cardiovascular Research Center, University of Missouri, Columbia, MO, 65212, USA

⁴Department of Medical Pharmacology and Physiology, University of Missouri School of Medicine, Columbia, MO, 65212, USA

⁵Department of Medicine, University of Missouri School of Medicine, Columbia, MO, 65212, USA

⁶INSERM, UMRS 1138, Cordeliers Research Center, Sorbonne University, USPC, Université Paris Descartes, Université Paris Diderot, F-75006, Paris, France

Abstract

Objective—Mineralocorticoid receptor activation of the epithelial sodium channel in endothelial cells (ECs) (EnNaC) is accompanied by aldosterone induced endothelial stiffening and impaired nitric oxide (NO)-mediated arterial relaxation. Recent data support enhanced activity of the alpha subunit of EnNaC (α EnNaC) mediates this aldosterone induced endothelial stiffening and associated endothelial NO synthase (eNOS) activation. There is mounting evidence that diet induced obesity diminishes expression and activation of AMP-activated protein kinase α (AMPK α), sirtuin 1 (Sirt1), which would be expected to lead to impaired downstream eNOS activation. Thereby, we posited that enhanced EnNaC activation contributes to diet induced obesity related increases in stiffness of the endothelium and diminished NO mediated vascular relaxation

***Corresponding Author:** Guanghong Jia, PhD, Assistant Professor of Medicine, Department of Medicine-Endocrinology, University of Missouri School of Medicine, D109 Diabetes Center HSC, One Hospital Drive, Columbia, MO 65212, Phone: (573) 884-0769; Fax: (573) 884-5530, Jiag@health.missouri.edu.

Author Contributions

Drs. Jia and Sowers contributed to the design of the study, and all authors were involved in data collection and analysis, data interpretation and manuscript writing.

Disclosure Statement

No relevant disclosures exist for this work.

Publisher's Disclaimer: This is a PDF file of an unedited manuscript that has been accepted for publication. As a service to our customers we are providing this early version of the manuscript. The manuscript will undergo copyediting, typesetting, and review of the resulting proof before it is published in its final form. Please note that during the production process errors may be discovered which could affect the content, and all legal disclaimers that apply to the journal pertain.

by increasing oxidative stress and related inhibition of AMPK α , Sirt1, and associated eNOS inactivation.

Materials/Methods—Sixteen to twenty week-old α EnNaC knockout (α EnNaC $^{-/-}$) and wild type littermate (EnNaC $^{+/+}$) female mice were fed a mouse chow or an obesogenic western diet (WD) containing excess fat (46%) and fructose (17.5%) for 16 weeks. Sodium currents of ECs, endothelial stiffness and NO mediated aortic relaxation were examined along with indices of aortic oxidative stress, vascular remodeling and fibrosis.

Results—Enhanced EnNaC activation-mediated WD-induced increases in sodium currents in isolated lung ECs, increased endothelial stiffness and impaired aortic endothelium-dependent relaxation to acetylcholine (10^{-9} – 10^{-4} mol/L). These abnormalities occurred in conjunction with WD-mediated aortic tissue oxidative stress, inflammation, and decreased activation of AMPK α , Sirt1, and downstream eNOS were substantially mitigated in α EnNaC $^{-/-}$ mice. Importantly, α EnNaC $^{-/-}$ prevented WD induced increases in endothelial stiffness and related impairment of endothelium-dependent relaxation as well as aortic fibrosis and remodeling. However, EnNaC signaling was not involved in diet-induced abnormal expression of adipokines and CYP11b2 in abdominal aortic perivascular adipose tissue.

Conclusion—These data suggest that endothelial specific EnNaC activation mediates WD-induced endothelial stiffness, impaired eNOS activation, aortic fibrosis and remodeling through increased aortic oxidative stress and increased inflammation related to a reduction of AMPK α and Sirt 1 mediated eNOS phosphorylation/activation and NO production.

Keywords

Obesity; endothelial sodium channels; nitric oxide; oxidative stress; fuel sensing kinases; endothelial stiffness

1. Introduction

Obesity is associated with increases in cardiovascular disease (CVD) and represents a rapidly growing health problem that has reached epidemic proportions [1, 2]. This epidemic is driven, in part, by consumption of a Western diet (WD) high in saturated fat and processed sugars, which may lead to vascular abnormalities characterized early by endothelial dysfunction and vascular stiffening [3]. Importantly, studies have shown that such increases in arterial stiffness during diet-induced obesity (DIO) usually occur prior to the development of hypertension [4, 5]. Further, data from the Framingham Heart Study show that increased arterial stiffening is an independent predictor of CVD in the general population, the elderly, and hypertensive patients [6]. A possible mechanism linking arterial stiffening with obesity is enhanced activation of vascular mineralocorticoid receptors (MRs) [5], which results in tissue inflammation, oxidative stress, reduced nitric oxide (NO) bioavailability, fibrosis and maladaptive remodeling [3, 7]. Recent data indicate that consumption of a WD or high fat diet increases plasma aldosterone levels [8, 9] and promotes vascular MR-mediated epithelial sodium channels (ENaC) in endothelial cell (EC) (EnNaC) activation, impaired endothelial NO synthase (eNOS) activation and EC stiffness [3, 7], suggesting that WD increased expression and activation of EnNaC through increased aldosterone and MR activation. It is interesting that these DIO mediated abnormalities characterizing EC stiffness

occur earlier and are more prominent in females than in males (3). However, there remains a gap in our understanding of the molecular signaling mechanisms by which DIO induces EnNaC mediated diminution of eNOS activation and related NO dependent vascular relaxation.

Arterial ECs maintain vascular homeostasis and normal physiological function partly through the actions of EC-derived NO [10]. Recent studies indicate that aldosterone induces EC MR-mediated activation of EnNaC which, in turn, leads to increased endothelial stiffness and impaired eNOS activation [7]. The α -EnNaC subunit is regarded as the core functional component of this heterotrimeric channel, with the β/γ -EnNaC subunits serving as amplifiers and modulators of the channel's activity [11, 12]. Increases in α EnNaC subunit expression and membrane abundance in ECs leads to enhanced inward sodium (Na^+) influx, polymerization of G-actin to F-actin (increases endothelial stiffness) and reduces EC eNOS activity and NO production [3, 7, 13]. Consistent with this notion, genetic depletion of the α EnNaC subunit (α EnNaC^{-/-}) decreased aldosterone mediated endothelial stiffness and impaired eNOS responses [7]. However, the potential mechanisms by which EnNaC in promoting obesity related impairment of eNOS activation and related arterial dysfunction has not been explored.

In this regard, DIO leads to suppression of the fuel sensing molecule 5' adenosine monophosphate-activated protein kinase alpha (AMPK α) and sirtuin 1 (Sirt1) signaling, which in turn, may lead to insulin resistance, endothelial dysfunction and impaired vascular relaxation [14, 15]. Indeed, AMPK α activation is necessary for phosphorylation and optimal activation of eNOS [16], and Sirt1 promotes phosphorylation/activation of eNOS through deacetylating lysine 496 and 506 [17]. Further, both increased AMPK α and Sirt1 can also repress tissue oxidative stress [17, 18] thereby promoting increased bioavailable NO.

Obese women have substantially increased vascular stiffness and lose the CVD protection normally afforded to non-obese females [5, 19, 20]. In line with these epidemiological observations in obese women, work in preclinical models indicate that female mice fed a WD become insulin resistant with a more rapid onset of vascular [21] and cardiac stiffness [20] compared to males. On the basis of the above, we hypothesized that enhanced EnNaC activation promotes WD-induced endothelial stiffness, impairs eNOS activation, and promotes aortic fibrosis and maladaptive vascular remodeling in females. We further posited that these adverse vascular effects are also promoted via increased inflammation and oxidative stress that are associated with a reduction in activation of AMPK α , Sirt1, and downstream eNOS phosphorylation/ activation.

2. Methods

All animal procedures were performed in accordance with National Institutes of Health Guide for the Care and Use of Laboratory Animals, the Animal Care and Use Committee at the University of Missouri-Columbia, and the Subcommittee for Animal Safety at the Truman VA Hospital/Center. α EnNaC^{-/-} mice were generated and crossed with Tie 2 Cre⁺ mice and wild-type littermates (α EnNaC^{+/+}) as described before [7, 22]. Sixteen to twenty

week-old $\alpha\text{EnNaC}^{-/-}$ and $\alpha\text{EnNaC}^{+/+}$ female mice were fed a standard mouse chow (CD) or a WD containing excess fat (46%) and fructose (17.5%) for a further 16 weeks.

2.1. Structural, biochemical parameters, and tail cuff blood pressure measurements

After 16 weeks of feeding, mice underwent body composition analysis for whole body fat mass, lean mass and total body water using an EchoMRI-500 for quantitative magnetic resonance analysis (Echo Medical Systems, Houston, TX, USA) as previously described [23]. Blood samples were collected from a subset of fasting mice in each treatment group and plasma was stored at -80°C for glucose and insulin assays and homeostatic model assessment of insulin resistance (HOMA-IR) [23]. Tail cuff blood pressure measurements protocols involved collection of several dozen measurements, with the software establishing the validity of each measurement. Data were tabulated in excel files and valid readings were used to calculate mean values for each mouse (Kent Scientific Corporation, Torrington, Conn., USA) [24].

2.2. Aortic stiffness by pulse wave velocity (PWV)

In vivo Doppler ultrasound (Indus Mouse Doppler System, Webster, TX) was performed on mice to determine PWV according to a previously established protocol [3]. In brief, the distance between two locations along the aorta was divided by the difference in arrival times and is expressed in m/s. Velocity wave forms were acquired at the aortic arch followed immediately by measurement at the descending aorta 35 mm distal to the aortic arch.

2.3. EC isolation and patch clamp

Mouse lungs were isolated and digested with collagenase IV for 90 minutes after which ECs were isolated by sequential passage across anti-CD45 antibody and anti-CD31 antibody-conjugated microbeads (Miltenyi Biotec Inc., Auburn, CA, USA) [3] and cultured for 5–8 days at 37°C , 5% CO_2 . Whole cell Na^+ currents were recorded by patch clamp using an EPC-10 amplifier (Heka) and Patchmaster and analyzed using Igor Pro software [25]. Patch pipette solution contained (in mM) 40 KCl, 100 K-gluconate, 1 CaCl_2 , 0.1 EGTA, 4 Na_2ATP , 10 Glucose, 10 Hepes, 2 GTP-Na_2 (pH 7.2 with KOH). Bath solution contains NaCl , 120, 4.5 KCl, 1.0 CaCl_2 , 1.0 MgCl_2 , 10 glucose, 10 Hepes (pH 7.2 with NaOH) [26]. Borosilicate glass pipette tip resistance ranged from 4.0 to 6.0 M when filled with intracellular solution. Whole-cell Na^+ currents were evoked by voltage steps delivered from holding potential of 0 mV to potentials ranging from -80 to $+80$ mV, in 40 mV increments. Series resistance ($<10\text{M}$) compensation was performed to minimize the duration of the capacitive surge. EnNaC currents were confirmed by inhibition with the Na^+ channel inhibitor, amiloride (1 μM). All experiments were performed at room temperature.

2.4. Atomic force microscopy (AFM) measurement of cell stiffness and ex vivo assessment of aortic reactivity

Stiffness of ECs was determined in intact mouse aortic explants using a nanoindentation AFM protocol as previously described [3]. For *ex vivo* assessment of reactivity of aortic rings contractile responses to KCl (80 $\text{mM}\cdot\text{L}^{-1}$) were measured using myography. To assess vasodilator capacity, aortic rings were precontracted with U46619 (30 nM) and relaxation

measured following cumulative addition of either acetylcholine (1 nM to 10 mM; endothelial dependent) or sodium nitroprusside (1 nM to 10 mM; endothelial independent).

2.5. Western-blot and quantitative PCR

Protein concentration of aortic tissue homogenates were measured as previously described [3]. To quantify specific proteins, western blots were incubated overnight at 4°C with primary antibodies against pSer-eNOS/eNOS (1:1000 dilution, #612393/#610297, BD Biosciences, San Jose, CA), pAMPK α /AMPK α (1:500 dilution, 2535s/2793, Cell signaling, Danvers, MA), Sirt1 (1:1000 dilution, 3931s, Cell signaling, Danvers, MA), GAPDH (1:2000 dilution, #5174s, Cell Signaling Technology, Danvers, MA). Bands were visualized by chemiluminescence, and images were recorded using a Bio-Rad ChemiDoc XRS image-analysis system. For quantitative PCR, first-strand cDNA synthesis was performed using 1 μ g total RNA with oligo dT (1 μ g), 5x reaction buffer, MgCl₂, dNTP mix, RNase inhibitor, and Improm II reverse transcriptase using an Improm II reverse transcription kit (Promega, Madison, WI). Real-time PCR was performed using 8 μ l cDNA, 10 μ l SYBR green PCR master mix (Bio-Rad Laboratories) and forward and reverse primers (10 pM/ μ l) (Integrated DNA Technologies, San Diego, CA) and a real-time PCR system (CFX96; Bio-Rad Laboratories).[3] Primer sequences used were: nicotinamide adenine dinucleotide phosphate (NADPH) oxidase 2 (NOX2), Forward: 5'-CTTTGGTACAGCCAGTGAAGA -3', Reverse: 5'-CCAGACAGACTTGAGAATGGAG -3'; Intercellular adhesion molecule-1 (ICAM-1), Forward: 5'-GTGATGGCAGCCTCTTATGT -3'; Reverse: 5'-GGGCTTGTCCTTGAGTTT-3'. Vascular cell adhesion molecule-1 (VCAM-1), Forward: 5'-GAGGGAGACACCGTCATTATC-3'; Reverse: 5'-CGAGCCATCCACAGACTTTA -3'. Interleukin 6 (IL6), Forward: 5'-CTTCCATCCAGTTGCCTTCT-3'; Reverse: 5'-CTCCGACTTGTGAAGTGGTATAG-3'. Monocyte chemoattractant protein 1 (MCP-1), Forward: 5'-GATGCAGTTAATGCCCCACT-3'; Reverse: 5'-TTCCTTATTGGGGTCAGCAC-3'. Leptin, Forward: 5'-CCTGTGGCTTTGGTCCTATC-3'; Reverse: 5'-GATCCTGGTGACAATGGTCTT-3'. Adiponectin, Forward: 5'-TGAGACAGGAGATGTTGGAATG-3'; Reverse: 5'-ACGCTGAGCGATACACATAAG-3'. CD11b, Forward: 5'-CCAAGACGATCTCAGCATCA-3'; Reverse: 5'-TTCTGGCTTGCTGAATCCTT-3'. CD206, Forward: 5'-CAAGGAAGGTTGGCATTGT- 3'; Reverse: 5'-CCTTTCAGTCCTTTGCAAGC-3'. CYP11b2, Forward: 5'-ATGCTCCTGCTTCACCATATAC-3'; Reverse: 5'-CTGGAGCTGGGCATCAAA-3'. ACE, Forward: 5'-GACAGGTTTCGTGGAAGAGTATG-3'; Reverse: 5'-TTGCTGCCCTCTATGGTAATG-3'. Endothelin-1 (ET-1), Forward: 5'-TGGTGAAGGAAGGAAACTAC-3'; Reverse: 5'-GCGTCAACTTCTGGTCTCTAT-3'. GAPDH, Forward: 5'-GGAGAAACCTGCCAAGTATGA-3', Reverse: 5'-TCCTCAGTGTAGCCCAAGA-3'. PCR protocols consisted of 5 min at 95°C for initial denaturation, 40 cycles of 30 s at 95°C, 30 s at 58°C and 30 s at 72°C. Results were normalized against the housekeeping gene, GAPDH.

2.6. Immunohistochemistry

Segments of thoracic aorta (approximately 2mm in length) were fixed in 3% paraformaldehyde, dehydrated in an ethanol series, paraffin embedded, and transversely sectioned (5 μ m slices). To evaluate fibrosis, aortic samples were stained with picro-sirus-red. Additional sections were incubated with antibodies to either 3-nitrotyrosine (3-NT) (Millipore, Billerica, MA) or collagen I (Abcam, Cambridge, MA) overnight at room temperature. Areas and the intensities of staining for 3-NT (brown color) and Collagen-1 (red color) were quantified using MetaVue.

2.7. Statistical analysis

Results are reported as means \pm SEM. Statistical differences were determined using one/two-way ANOVA multiple comparison analyses and Gabriel Students-Newman-Keuls post-test. Differences were considered significant at $p < 0.05$. All statistical analyses were performed using Sigma Plot (version 12) software (Systat Software, San Jose, CA).

3. Results

3.1. Effects of WD on characteristics of α EnNaC^{+/+} and α EnNaC^{-/-} mice

We have previously observed that our WD induces weight gain and fat mass without significant alterations in blood pressure [3, 23]. In the present study, there were no significant differences in fat mass, body weight, peri-reproductive fat mass and blood pressure (BP) between CD α EnNaC^{-/-} and their littermate controls (Table 1). Compared to CD-fed mice, 16 weeks of WD induced 1.91, 1.15, and 1.51 fold increases in whole body fat mass, body weight, and peri-reproductive fat mass, respectively ($p < 0.05$) (Table 1). In contrast, there were no significant differences in body fat mass, body weight and peri-reproductive fat mass between α EnNaC^{+/+} vs α EnNaC^{-/-} mice after consuming the WD. Of note, there were also no significant differences in lean mass, retro-peritoneal fat, cholesterol, triglycerides, fasting glucose, homeostatic model assessment-insulin resistance (HOMA-IR), systolic BP, diastolic BP, or pulse pressure between any of the groups (Table 1).

3.2. α EnNaC^{-/-} prevents WD-induced increases of EC inward Na⁺ currents

Our previous data demonstrated that the ENaC antagonist, amiloride (1 μ mol), inhibits inward EC Na⁺ currents, *in vitro* [7]. To evaluate the effect of WD on EC Na⁺ currents from α EnNaC^{+/+} and α EnNaC^{-/-} mice, lung ECs from the experimental groups were isolated and Na⁺ currents measured by patch clamp [7]. Following 16 weeks of WD feeding a significant increase in inward Na⁺ current was observed in lung ECs isolated from α EnNaC^{+/+} mice compared to those of mice fed the CD (Fig. 1A–C). In contrast, EC Na⁺ currents of α EnNaC^{-/-} mice fed the WD were attenuated compared to those of α EnNaC^{+/+} mice consuming a WD (Fig. 1B–C). These data suggest that the α EnNaC subunit is required for channel activation and the subsequent increase in EC Na⁺ currents that occurs in response to WD feeding.

3.3 α EnNaC^{-/-} prevents WD-Induced increases in endothelial stiffness and impaired NO mediated aortic relaxation

α EnNaC^{+/+} mice fed the WD (16 weeks) exhibited increased endothelial stiffness, measured *ex vivo*, while *in vivo* PWV (measure of whole vessel stiffness) was unaltered (Fig. 2A–B). The diet-induced increase in *ex vivo* aortic endothelial stiffness was, however, significantly blunted in α EnNaC^{-/-} mice (Fig. 2A–B). Similarly, WD feeding impaired aortic endothelium (NO)-dependent relaxation to acetylcholine that was significantly attenuated in α EnNaC^{-/-} mice (Fig. 2C). In contrast, no significant differences were observed between groups in response to the endothelium-independent vasodilator, sodium nitroprusside (Fig. 2D). Collectively these data indicate a role for EnNaC activation in WD-induced increases in endothelial stiffness, reduced eNOS activation and associated impaired endothelium-dependent relaxation.

3.4. α EnNaC^{-/-} prevents WD-induced aortic oxidative stress

To determine the role of EnNaC in WD-induced aortic oxidative stress, we evaluated 3-NT production and levels of NOX2 mRNA expression. The α EnNaC^{+/+} mice fed the WD (16 weeks) showed significantly increased levels of 3-NT and NOX2 mRNA expression (Fig. 3A–C). Importantly, α EnNaC deletion attenuated the WD-induced increase in both 3-NT production and NOX2 expression (Fig. 3).

3.5. α EnNaC^{-/-} prevents WD-induced inflammation and reductions in AMPK α and Sirt1 and downstream eNOS activity

In addition to increasing aortic oxidative stress, 16 weeks consumption of a WD increased mRNA levels of VCAM-1 and MCP-1 but not ICAM-1 and IL6 (Fig 4A). Consumption of the WD was also associated with reduced phosphorylation/activation of AMPK α and eNOS as well as decreased expression of Sirt1 (Fig 4). Again, these impairments were significantly blunted in α EnNaC^{-/-} mice (Fig 4), consistent with the notion that EnNaC activation is critical for WD-induced increases in oxidative stress, inflammation, and inhibition of AMPK α and Sirt1 and resultant reductions in eNOS activity.

3.6. α EnNaC^{-/-} prevents WD-induced aortic fibrosis and remodeling

Consistent with previous studies, consumption of a WD in EnNaC^{+/+} mice increased aortic fibrosis as shown by picro-sirius red staining. The diet-induced increase in aortic fibrosis was significantly attenuated in α EnNaC^{-/-} mice (Fig. 5). Compared to WD α EnNaC^{+/+} mice, expression of collagen I was concomitantly decreased in α EnNaC^{-/-} mice consuming the obesogenic diet (Fig 5).

3.7. α EnNaC deletion in mice does not prevent WD-induced increases in inflammation and CYP11b2 in abdominal aortic perivascular adipose tissue (PVAT)

Fat tissues release adipokines, leptin, adiponectin, macrophage M1 markers CD11b and IL6, as well as M2 marker CD206 [27]. Consumption of a WD in EnNaC^{+/+} mice increased mRNA levels of leptin, macrophage M1 markers CD11b and IL6, which were not significantly attenuated in α EnNaC^{-/-} mice (Fig. 6A). Meanwhile, DIO also induced an increase of CYP11b2 (aldosterone synthase) expression, and this was not significantly

inhibited in $\alpha\text{EnNaC}^{-/-}$ mice in abdominal aortic PVAT (Fig 6B). There were no significant differences in mRNA levels of adiponectin CD206, ACE and ET-1 between any of the groups (Fig 6).

4. Discussion

This investigation provides several novel findings that advance our understanding of the role played by the endothelial Na^+ channel in the development of increased endothelial stiffness and impaired NO mediated vascular relaxation associated with DIO. First, consumption of the WD increased inward Na^+ currents in isolated ECs. Secondly, the enhanced EC Na^+ currents were associated with significant increases in aortic oxidative stress characterized by increased 3-NT levels and NOX2 expression as well as the markers of inflammation, VCAM-1 and MCP-1. Thirdly, consumption of a WD inhibited activation (phosphorylation) of AMPK α and eNOS and Sirt1 expression. These WD induced EC abnormalities were associated with increased endothelial stiffness, impaired NO-dependent relaxation, aortic fibrosis and remodeling. Importantly, these endothelial abnormalities occurring in response to WD feeding were significantly attenuated in $\alpha\text{EnNaC}^{-/-}$ mice implicating a central role for endothelial Na^+ channel activation. Lastly, endothelium specific ENaC signaling was not involved in diet-induced abnormal release of adipokines and CYP11b2 in abdominal aortic PVAT.

The epithelial Na^+ channel, ENaC, is a heterotrimeric ion channel consisting of α , β , γ , and δ subunits. These subunits have been reported in a variety of cell types, including most recently in ECs [12, 28–30]. The α -ENaC subunit is regarded as the core channel forming component while the β/γ -ENaC subunits serve as amplifiers and modulators of the channel's activity [11, 12]. An important role for the α subunit of ENaC in vascular function is supported by this subunit being critical for the regulation of flow-mediated vascular dilation through a shear-stress sensing mechanism [3, 22]. Further, increased expression, membrane localization and activation of the αEnNaC subunit contributes to EC stiffness *in vitro* in human and mouse ECs, as well as in the Liddle syndrome mouse model [7, 11]. Our current data for the first time support a critical role for the α subunit and activation of ENaC in enhancing inward Na^+ currents which then lead to increases in EC stiffness and impaired eNOS activation, oxidative stress and inflammation in the setting of DIO.

Previous studies have shown that DIO is associated with increased plasma aldosterone levels [8, 9], as well as enhanced activation of the vascular endothelial MR leading to ENaC activation. This, in turn, promoted Na^+ entry into ECs which induced polymerization of G-actin to F-actin [3, 7]. Such cytoskeletal remodeling is thought to repress calveolar eNOS activity which reduces NO production, resulting in EC remodeling of the actin cytoskeleton and excessive endothelium stiffness [3, 29, 31].

Our recent studies have shown that *in vivo* global inhibition of ENaC with amiloride [21] and EC specific deletion of $\alpha\text{EnNaC}^{-/-}$ [7] prevents MR mediated arterial stiffness and improves flow-induced resistant artery dilation. In the current investigation the $\alpha\text{EnNaC}^{-/-}$

genotype prevented WD-induced endothelium stiffness and associated impairment of eNOS activation.

WD consumption by rodents has been shown to increase aortic oxidative stress which is regarded as an important contributor to obesity related EC dysfunction and adverse arterial remodeling [32, 33]. Evidence from studies of both rodents [34, 35] and humans [36, 37] suggests that dietary manipulations, including a high salt diet, induce oxidative stress which subsequently increases ENaC activity in kidney epithelial cells [38]. Oxidative stress (for example H₂O₂-induced) has also been shown to increase lung α ENaC expression and activity via inhibitory effects on ubiquitin-like protein Nedd8 [39]. Accordingly, increased oxidative stress likely promotes inward EC Na⁺ currents and endothelial stiffness and impaired eNOS activation. Indeed, in dendritic cells, the α/β subunits of ENaC mediate high Na⁺-induced activation of p47^{phox}, gp91^{phox} and oxidative stress through activation of the Na⁺/Ca²⁺ exchanger and protein kinase C [40]. Our recent data showed that endothelial specific α EnNaC deletion mitigates aldosterone-induced endoplasmic reticulum stress and NOX2 mediated oxidative stress, as well as pro-inflammatory responses [7]. Consistent with these findings, our current data further demonstrate that EnNaC activation mediates diet-induced obesity related increases in 3-NT, VCAM-1 and MCP-1, oxidative stress inflammation and impaired eNOS activation.

DIO plays an important role in development of arterial stiffness through abnormal release of IL-6, IL-8, and inflammation adhesion molecules in aorta [1]. Our recent data indicates that EnNaC mediates chronic aldosterone infusion-increased endothelium permeability and subsequent elevated CD68, IL1 and IL6 [7]. In the current study, the data indicates that EnNaC activation mediates WD-induced increases in the proinflammation cytokines VCAM-1 and MCP-1. Meanwhile, diet and other factors regulate fuel presentation to cells, thereby modulating AMPK α , Sirt1 and eNOS activity, in part, through changes in oxidative stress [41]. To this point, increased oxidative stress in obesity inhibits AMPK activity through inhibition of liver kinase B1 activity [42]. Both oxidative and endoplasmic reticulum stress can also diminish AMPK activity [43, 44]. Conversely, inhibition of oxLDL-induced oxidative stress significantly increases the phosphorylation and activation of AMPK α in vitro [45]. AMPK α activation is important in both stimulation of eNOS activity and anti-oxidative effects. For instance, activation of AMPK α induces an increase of phosphorylation of eNOS at Ser1177, and the resultant eNOS activation leads to increases in NO production in human aorta ECs [46]. AMPK α deficiency also increases the expression of p47^{phox}, p67^{phox}, and gp91^{phox} and consequent NADPH oxidase activation in human umbilical vein ECs [47]. The resultant increases in oxidative stress, in turn, leads to increases in NO destruction [47]. Thus, a deficiency of AMPK α induced by diet-induced obesity, as occurred in the present study, would be expected to decrease bioavailable NO by reducing eNOS activation and increasing oxidative stress mediated NO destruction.

While increases in Sirt1, acting via its deacetylase activity, have been shown to increase expression and activation of eNOS, increased eNOS activation and NO production, in turn, also stimulates Sirt1 expression [48, 49]. Conversely, increases in expression of the NADPH subunit p22 (phox) and NADPH oxidase activity, and resulting vascular superoxide production, have been shown to inhibit Sirt1 expression and endothelium (NO)-dependent

relaxation [50]. Our present data are consistent with the notion that EnNaC-mediated oxidative stress is associated with increased EC stiffness and impaired NO mediated relaxation through reduction of expression of Sirt1 and activation of AMPK α and downstream activation of eNOS, as well as NO destruction by the increased oxidant moieties. The resulting reduction in bioavailable NO has been shown to enhance collagen crosslinking and promote aortic fibrosis as observed in this study of mice consuming a WD [50].

It is important to note that there were no differences in baseline physiological parameters such as BP and aortic relaxation between control α EnNaC^{+/+} and α EnNaC^{-/-} mice. While EnNaC contributes to the maintenance of normal endothelium function its deletion does not appear to lead to a significant abnormal arterial phenotype, under control conditions (i.e. with consumption of normal chow diet). Another factor may be that at this relatively early stage of feeding in this study other compensatory mechanism affect in vivo arterial hemodynamics. Indeed, a prior study showed that inhibition of ENaC with benzamil blunted acetylcholine-induced NO production in mesenteric arteries from wild type mice but not in α EnNaC^{-/-} mice, suggesting a role for endothelial EnNaC in acetylcholine-induced NO production under normal physiological circumstances [22]. This is further confirmed in the current study as Sirt1 was decreased in control α EnNaC^{-/-} since Sirt1 is related to NO production. Therefore, the effects of EnNaC on vascular function appear to be different and under pathological (ie DIO) versus physiological conditions. Further, the current investigation shows that while WD induced EC stiffness and impaired eNOS activation, it did not result in an increased PWV and aortic stiffness. Similar results were found in our recent study which showed that 3 weeks of aldosterone infusion did not increase PWV in EnNaC^{+/+} control mice [7]. Indeed, increased aortic stiffness involves the dysfunction of not only the EC, but also vascular smooth muscle cells and extracellular matrix stiffness [33]. Thus, we suggest that development of endothelial stiffness and associated reductions in NO production precedes and is a necessary precursor to the development of aortic stiffness as determined by increased PWV.

Fat tissue has been shown to be associated with abnormalities in the production/action of adipokines and endothelium-derived contracting factors [27]. Data from this study support this notion as DIO increased mRNA levels of leptin and macrophage M1 markers CD11b and IL6 in aortic PVAT. DIO also increased aortic PVAT mRNA for CYP11 b2 that is related to aldosterone production. Consistent with this, our previous data showed that WD feeding leads to elevated plasma aldosterone levels [8] and vascular MR activation [3], which are both involved in impaired endothelium dependent artery relaxation [3, 8]. However, deletion of α EnNaC did not prevent the WD-induced increases in inflammation and CYP11b2 in abdominal aortic PVAT, suggesting endothelium specific EnNaC signaling is not involved in abnormal production/action of adipokines and vascular contracting factors in arterial PVAT.

It is important to acknowledge that the current studies focused on female mice. The rationale for having chosen female mice related to the observation that obese and diabetic females lose CVD protection that is typically afforded by female sex and this may relate to an increased propensity to develop CV stiffness in obese females [20]. This notion is supported in our previous work where C57BL6J mice fed a WD showing that female mice display a

more rapid onset of insulin resistance as well as aortic [21] and cardiac stiffness [20] compared to males. In addition, the elevation in plasma aldosterone levels induced by consumption of a WD is higher in females compared to males [20]. We intend to further examine the gender difference in diet-induced vascular stiffness and its molecular mechanisms in future studies.

Collectively, we extend previous observations regarding the critical role for the α EnNaC subunit activation in the development of endothelial stiffness and reduced eNOS activation [7, 21]. This investigation also uncovered mechanisms by which excess nutrient intake leads to diminished vascular eNOS activation. Data from this investigation further indicates that consumption of a WD increases EnNaC activity, which subsequently leads to increased oxidative stress, inflammation, and associated increased endothelium stiffness and impaired NO mediated aortic relaxation (Fig 7). Our data suggest that this DIO induced diminution of eNOS activation occurs, in part, via reduced activation of the nutrient sensitive molecules AMPK α and Sirt1.

In summary, abnormally increased EC stiffness appears to be a critical early instigator of vascular disease since mechanical stiffening of the ECs causes impaired NO production that typically precede whole arterial structural and functional abnormalities and hypertension. Interventions that prevent or mitigate endothelial stiffness offer a potential therapeutic strategy in the prevention and early treatment of vascular stiffness and associated impairment of relaxation associated with obesity in females.

Acknowledgments

We acknowledge the work by Dr. Vincent G. DeMarco, who did and analyzed PWV data. We also acknowledge Matthew B. Martin and Dongqing Chen for their help in animal experiments and Ernesto Martinez-Martinez for assistance in transfer of α EnNaC^{-/-} and littermate mice. This work was supported with resources and the use of facilities at the Harry S Truman Memorial Veterans Hospital in Columbia, MO.

Funding

Dr. Jia received funding from American Diabetes Association (Innovative Basic Science Award #1-17-IBS-201). JRS received funding from NIH (R01 HL73101-01A and R01 HL107910-01). Dr. Whaley-Connell received funding from the Veterans Affairs Merit System (BX003391). Dr. Hill received funding from NIH (R01HL085119). Dr. Sowers and Lastra received funding from the Veterans Affairs Merit System (2I01BX001981-05A1). Dr Jaisser received funding from the Fondation de France (2014-00047968) and ANR Investissement Avenir CARMMA (ANR15-RHUS-0003).

Abbreviations

CVD	cardiovascular disease
WD	Western diet
DIO	Diet-induced obesity
MR	mineralocorticoid receptor
NO	nitric oxide
EC	endothelial cell

Na⁺	Sodium
αENaC	epithelial Na ⁺ channel alpha
αEnNaC	αENaC in ECs
eNOS	endothelial NO synthase
AMPKα	5' adenosine monophosphate-activated protein kinase alpha
Sirt1	sirtuin 1
Bp	blood pressure
PWV	pulse wave velocity
PVAT	perivascular adipose tissue
3-NT	3-Nitrotyrosine
NOXs	nicotinamide adenine dinucleotide phosphate oxidase
VCAM-1	vascular cell adhesion molecule-1
ICAM-1	intercellular adhesion molecule-1
MCP-1	monocyte chemoattractant protein 1
IL6	interleukin 6

References

- [1]. Koliaki C, Liatis S, Kokkinos A. Obesity and cardiovascular disease: revisiting an old relationship. *Metabolism* 2019;92:98–107. Epub 2018/11/07. doi: 10.1016/j.metabol.2018.10.011. [PubMed: 30399375]
- [2]. Polyzos SA, Kountouras J, Mantzoros CS. Obesity and nonalcoholic fatty liver disease: From pathophysiology to therapeutics. *Metabolism* 2019;92:82–97. Epub 2018/12/07. doi: 10.1016/j.metabol.2018.11.014. [PubMed: 30502373]
- [3]. Jia G, Habibi J, Aroor AR, Martinez-Lemus LA, DeMarco VG, Ramirez-Perez FI, et al. Endothelial Mineralocorticoid Receptor Mediates Diet-Induced Aortic Stiffness in Females. *Circ Res* 2016;118(6):935–43. doi: 10.1161/CIRCRESAHA.115.308269. [PubMed: 26879229]
- [4]. Weisbrod RM, Shiang T, Al Sayah L, Fry JL, Bajpai S, Reinhart-King CA, et al. Arterial stiffening precedes systolic hypertension in diet-induced obesity. *Hypertension* 2013;62(6):1105–10. doi: 10.1161/HYPERTENSIONAHA.113.01744. [PubMed: 24060894]
- [5]. DeMarco VG, Habibi J, Jia G, Aroor AR, Ramirez-Perez FI, Martinez-Lemus LA, et al. Low-Dose Mineralocorticoid Receptor Blockade Prevents Western Diet-Induced Arterial Stiffening in Female Mice. *Hypertension* 2015;66(1):99–107. doi: 10.1161/HYPERTENSIONAHA.115.05674. [PubMed: 26015449]
- [6]. Mitchell GF, Hwang SJ, Vasan RS, Larson MG, Pencina MJ, Hamburg NM, et al. Arterial stiffness and cardiovascular events: the Framingham Heart Study. *Circulation* 2010;121(4):505–11. doi: 10.1161/CIRCULATIONAHA.109.886655. [PubMed: 20083680]
- [7]. Jia G, Habibi J, Aroor AR, Hill MA, Yang Y, Whaley-Connell A, et al. Epithelial Sodium Channel in Aldosterone-Induced Endothelium Stiffness and Aortic Dysfunction. *Hypertension* 2018;72(3):731–8. doi: 10.1161/HYPERTENSIONAHA.118.11339. [PubMed: 29987101]

- [8]. Aroor AR, Habibi J, Nistala R, Ramirez-Perez FI, Martinez-Lemus LA, Jaffe IZ, et al. Diet-Induced Obesity Promotes Kidney Endothelial Stiffening and Fibrosis Dependent on the Endothelial Mineralocorticoid Receptor. *Hypertension* 2019;73(4):849–858. doi: 10.1161/HYPERTENSIONAHA.118.12198. [PubMed: 30827147]
- [9]. Schafer N, Lohmann C, Winnik S, van Tits LJ, Miranda MX, Vergopoulos A, et al. Endothelial mineralocorticoid receptor activation mediates endothelial dysfunction in diet-induced obesity. *Eur Heart J* 2013;34(45):3515–24. doi: 10.1093/eurheartj/ehh095. [PubMed: 23594590]
- [10]. Zhao Y, Li N, Li Z, Zhang D, Chen L, Yao Z, et al. Conditioned medium from contracting skeletal muscle cells reverses insulin resistance and dysfunction of endothelial cells. *Metabolism* 2018;82:36–46. Epub 2018/01/01. doi: 10.1016/j.metabol.2017.12.008. [PubMed: 29289515]
- [11]. Jeggle P, Callies C, Tarjus A, Fassot C, Fels J, Oberleithner H, et al. Epithelial sodium channel stiffens the vascular endothelium in vitro and in Liddle mice. *Hypertension* 2013; 61 (5):1053–9. doi: 10.1161/HYPERTENSIONAHA.111.199455. [PubMed: 23460285]
- [12]. Li Q, Fung E. Multifaceted Functions of Epithelial Na(+) Channel in Modulating Blood Pressure. *Hypertension* 2019;73(2):273–81. doi: 10.1161/HYPERTENSIONAHA.118.12330. [PubMed: 30580685]
- [13]. Jia G, Habibi J, Aroor AR, Hill MA, DeMarco VG, Lee LE, et al. Enhanced endothelium epithelial sodium channel signaling prompts left ventricular diastolic dysfunction in obese female mice. *Metabolism* 2018;78:69–79. Epub 2017/09/19. doi: 10.1016/j.metabol.2017.08.008. [PubMed: 28920862]
- [14]. Yan M, Qi H, Xia T, Zhao X, Wang W, Wang Z, et al. Metabolomics profiling of metformin-mediated metabolic reprogramming bypassing AMPKalpha. *Metabolism* 2019;91:18–29. Epub 2018/11/24. doi: 10.1016/j.metabol.2018.11.010. [PubMed: 30468782]
- [15]. Thomas D, Apovian C. Macrophage functions in lean and obese adipose tissue. *Metabolism* 2017;72:120–43. Epub 2017/06/24. doi: 10.1016/j.metabol.2017.04.005. [PubMed: 28641779]
- [16]. Chen Z, Peng IC, Sun W, Su MI, Hsu PH, Fu Y, et al. AMP-activated protein kinase functionally phosphorylates endothelial nitric oxide synthase Ser633. *Circ Res* 2009;104(4):496–505. doi: 10.1161/CIRCRESAHA.108.187567. [PubMed: 19131647]
- [17]. Zhang W, Huang Q, Zeng Z, Wu J, Zhang Y, Chen Z. Sirt1 Inhibits Oxidative Stress in Vascular Endothelial Cells. *Oxid Med Cell Longev* 2017;2017:7543973. doi: 10.1155/2017/7543973. [PubMed: 28546854]
- [18]. Lefranc C, Friederich-Persson M, Braud L, Palacios-Ramirez R, Karlsson S, Boujardine N, et al. MR (Mineralocorticoid Receptor) Induces Adipose Tissue Senescence and Mitochondrial Dysfunction Leading to Vascular Dysfunction in Obesity. *Hypertension* 2019;73(2):458–68. doi: 10.1161/HYPERTENSIONAHA.118.11873. [PubMed: 30624990]
- [19]. Regnault V, Thomas F, Safar ME, Osborne-Pellegrin M, Khalil RA, Pannier B, et al. Sex difference in cardiovascular risk: role of pulse pressure amplification. *J Am Coll Cardiol* 2012;59(20):1771–7. doi: 10.1016/j.jacc.2012.01.044. [PubMed: 22575315]
- [20]. Manrique C, DeMarco VG, Aroor AR, Mugerfeld I, Garro M, Habibi J, et al. Obesity and insulin resistance induce early development of diastolic dysfunction in young female mice fed a Western diet. *Endocrinology* 2013;154(10):3632–42. doi: 10.1210/en.2013-1256. [PubMed: 23885014]
- [21]. Martinez-Lemus LA, Aroor AR, Ramirez-Perez FI, Jia G, Habibi J, DeMarco VG, et al. Amiloride Improves Endothelial Function and Reduces Vascular Stiffness in Female Mice Fed a Western Diet. *Front Physiol* 2017;8:456. doi: 10.3389/fphys.2017.00456. [PubMed: 28713285]
- [22]. Tarjus A, Maase M, Jeggle P, Martinez-Martinez E, Fassot C, Loufrani L, et al. The endothelial alphaENaC contributes to vascular endothelial function in vivo. *PLoS One* 2017;12(9):e0185319. doi: 10.1371/journal.pone.0185319. [PubMed: 28950003]
- [23]. Jia G, Habibi J, Bostick BP, Ma L, DeMarco VG, Aroor AR, et al. Uric acid promotes left ventricular diastolic dysfunction in mice fed a Western diet. *Hypertension* 2015;65(3):531–9. doi: 10.1161/HYPERTENSIONAHA.114.04737. [PubMed: 25489061]
- [24]. Manrique C, Lastra G, Habibi J, Mugerfeld I, Garro M, Sowers JR. Loss of Estrogen Receptor alpha Signaling Leads to Insulin Resistance and Obesity in Young and Adult Female Mice. *Cardiorenal Med* 2012;2(3):200–10. doi: 000339563. [PubMed: 22969776]

- [25]. Yang Y, Sohma Y, Nourian Z, Ella SR, Li M, Stupica A, et al. Mechanisms underlying regional differences in the Ca²⁺ sensitivity of BK(Ca) current in arteriolar smooth muscle. *J Physiol* 2013;591(5):1277–93. doi: 10.1113/jphysiol.2012.241562. [PubMed: 23297302]
- [26]. Guo D, Liang S, Wang S, Tang C, Yao B, Wan W, et al. Role of epithelial Na⁺ channels in endothelial function. *J Cell Sci* 2016;129(2):290–7. doi: 10.1242/jcs.168831. [PubMed: 26621031]
- [27]. Jia G, Aroor AR, Sowers JR. The role of mineralocorticoid receptor signaling in the cross-talk between adipose tissue and the vascular wall. *Cardiovasc Res* 2017;113(9):1055–63. Epub 2017/08/26. doi: 10.1093/cvr/cvx097. [PubMed: 28838041]
- [28]. Wang S, Meng F, Mohan S, Champaneri B, Gu Y. Functional ENaC channels expressed in endothelial cells: a new candidate for mediating shear force. *Microcirculation* 2009;16(3):276–87. doi: 10.1080/10739680802653150. [PubMed: 19225981]
- [29]. Kusche-Vihrog K, Callies C, Fels J, Oberleithner H. The epithelial sodium channel (ENaC): Mediator of the aldosterone response in the vascular endothelium? *Steroids* 2010;75(8–9):544–9. doi: 10.1016/j.steroids.2009.09.003. [PubMed: 19778545]
- [30]. Czikora I, Alli AA, Sridhar S, Matthay MA, Pillich H, Hudel M, et al. Epithelial Sodium Channel- α Mediates the Protective Effect of the TNF-Derived TIP Peptide in Pneumolysin-Induced Endothelial Barrier Dysfunction. *Front Immunol* 2017;8:842. doi: 10.3389/fimmu.2017.00842. [PubMed: 28785264]
- [31]. Fels J, Jeggle P, Kusche-Vihrog K, Oberleithner H. Cortical actin nanodynamics determines nitric oxide release in vascular endothelium. *PLoS One* 2012;7(7):e41520. doi: 10.1371/journal.pone.0041520. [PubMed: 22844486]
- [32]. DuPont JJ, Jaffe IZ. 30 YEARS OF THE MINERALOCORTICOID RECEPTOR: The role of the mineralocorticoid receptor in the vasculature. *J Endocrinol* 2017;234(1):T67–T82. doi: 10.1530/JOE-17-0009. [PubMed: 28634267]
- [33]. Jia G, Aroor AR, Hill MA, Sowers JR. Role of Renin-Angiotensin-Aldosterone System Activation in Promoting Cardiovascular Fibrosis and Stiffness. *Hypertension* 2018;72(3):537–48. doi: 10.1161/HYPERTENSIONAHA.118.11065. [PubMed: 29987104]
- [34]. Cowley AW Jr. Renal medullary oxidative stress, pressure-natriuresis, and hypertension. *Hypertension* 2008;52(5):777–86. doi: 10.1161/HYPERTENSIONAHA.107.092858. [PubMed: 18852392]
- [35]. Jin C, Hu C, Polichnowski A, Mori T, Skelton M, Ito S, et al. Effects of renal perfusion pressure on renal medullary hydrogen peroxide and nitric oxide production. *Hypertension* 2009;53(6):1048–53. doi: 10.1161/HYPERTENSIONAHA.109.128827. [PubMed: 19433780]
- [36]. Lacy F, Kailasam MT, O'Connor DT, Schmid-Schonbein GW, Parmer RJ. Plasma hydrogen peroxide production in human essential hypertension: role of heredity, gender, and ethnicity. *Hypertension* 2000;36(5):878–84. [PubMed: 11082160]
- [37]. Redon J, Oliva MR, Tormos C, Giner V, Chaves J, Iradi A, et al. Antioxidant activities and oxidative stress byproducts in human hypertension. *Hypertension* 2003;41(5):1096–101. doi: 10.1161/01.HYP.0000068370.21009.38. [PubMed: 12707286]
- [38]. Ma HP. Hydrogen peroxide stimulates the epithelial sodium channel through a phosphatidylinositol 3-kinase-dependent pathway. *J Biol Chem* 2011;286(37):32444–53. doi: 10.1074/jbc.M111.254102. [PubMed: 21795700]
- [39]. Downs CA, Kumar A, Kreiner LH, Johnson NM, Helms MN. H₂O₂ regulates lung epithelial sodium channel (ENaC) via ubiquitin-like protein Nedd8. *J Biol Chem* 2013;288(12):8136–45. doi: 10.1074/jbc.M112.389536. [PubMed: 23362276]
- [40]. Barbaro NR, Foss JD, Kryshtal DO, Tsyba N, Kumaresan S, Xiao L, et al. Dendritic Cell Amiloride-Sensitive Channels Mediate Sodium-Induced Inflammation and Hypertension. *Cell Rep* 2017;21(4):1009–20. doi: 10.1016/j.celrep.2017.10.002. [PubMed: 29069584]
- [41]. Fruhbeck G, Gomez-Ambrosi J, Rodriguez A, Ramirez B, Valenti V, Moncada R, et al. Novel protective role of kallistatin in obesity by limiting adipose tissue low grade inflammation and oxidative stress. *Metabolism* 2018;87:123–35. Epub 2018/04/22. doi: 10.1016/j.metabol.2018.04.004. [PubMed: 29679615]

- [42]. Zhang Z, Wang S, Zhou S, Yan X, Wang Y, Chen J, et al. Sulforaphane prevents the development of cardiomyopathy in type 2 diabetic mice probably by reversing oxidative stress-induced inhibition of LKB1/AMPK pathway. *J Mol Cell Cardiol* 2014;77:42–52. doi: 10.1016/j.yjmcc.2014.09.022. [PubMed: 25268649]
- [43]. Dolinsky VW, Chan AY, Robillard Frayne I, Light PE, Des Rosiers C, Dyck JR. Resveratrol prevents the prohypertrophic effects of oxidative stress on LKB1. *Circulation* 2009;119(12):1643–52. doi: 10.1161/CIRCULATIONAHA.108.787440. [PubMed: 19289642]
- [44]. Choudhury M, Qadri I, Rahman SM, Schroeder-Gloeckler J, Janssen RC, Friedman JE. C/EBPbeta is AMP kinase sensitive and up-regulates PEPCK in response to ER stress in hepatoma cells. *Mol Cell Endocrinol* 2011;331 (1):102–8. doi: 10.1016/j.mce.2010.08.014. [PubMed: 20797423]
- [45]. Tsai KL, Hung CH, Chan SH, Shih JY, Cheng YH, Tsai YJ, et al. Baicalein protects against oxLDL-caused oxidative stress and inflammation by modulation of AMPK-alpha. *Oncotarget* 2016;7(45):72458–68. doi: 10.18632/oncotarget.12788. [PubMed: 27776344]
- [46]. Morrow VA, Fougelle F, Connell JM, Petrie JR, Gould GW, Salt IP. Direct activation of AMP-activated protein kinase stimulates nitric-oxide synthesis in human aortic endothelial cells. *J Biol Chem* 2003;278(34):31629–39. doi: 10.1074/jbc.M212831200. [PubMed: 12791703]
- [47]. Wang S, Zhang M, Liang B, Xu J, Xie Z, Liu C, et al. AMPKalpha2 deletion causes aberrant expression and activation of NAD(P)H oxidase and consequent endothelial dysfunction in vivo: role of 26S proteasomes. *Circ Res* 2010;106(6):1117–28. doi: 10.1161/CIRCRESAHA.109.212530. [PubMed: 20167927]
- [48]. Xia N, Strand S, Schlufte F, Siuda D, Reifenberg G, Kleinert H, et al. Role of SIRT1 and FOXO factors in eNOS transcriptional activation by resveratrol. *Nitric Oxide* 2013;32:29–35. doi: 10.1016/j.niox.2013.04.001. [PubMed: 23583951]
- [49]. Mattagajasingh I, Kim CS, Naqvi A, Yamamori T, Hoffman TA, Jung SB, et al. SIRT1 promotes endothelium-dependent vascular relaxation by activating endothelial nitric oxide synthase. *Proc Natl Acad Sci U S A* 2007;104(37):14855–60. doi: 10.1073/pnas.0704329104. [PubMed: 17785417]
- [50]. Zarzuelo MJ, Lopez-Sepulveda R, Sanchez M, Romero M, Gomez-Guzman M, Ungvary Z, et al. SIRT1 inhibits NADPH oxidase activation and protects endothelial function in the rat aorta: implications for vascular aging. *Biochem Pharmacol* 2013;85(9):1288–96. doi: 10.1016/j.bcp.2013.02.015. [PubMed: 23422569]

Highlights

- EnNaC is critical for development of endothelium stiffness and aortic dysfunction.
- Consumption of a WD promotes EC Na⁺ inward currents, oxidative stress, inflammation, endothelium stiffness, aortic fibrosis, remodeling and dysfunction through reduced activation of AMPK α , Sirt1 and eNOS.
- Blockade of EnNaC represents a potential therapeutic strategy for ameliorating the detrimental effects of obesity-induced arterial stiffness and dysfunction.

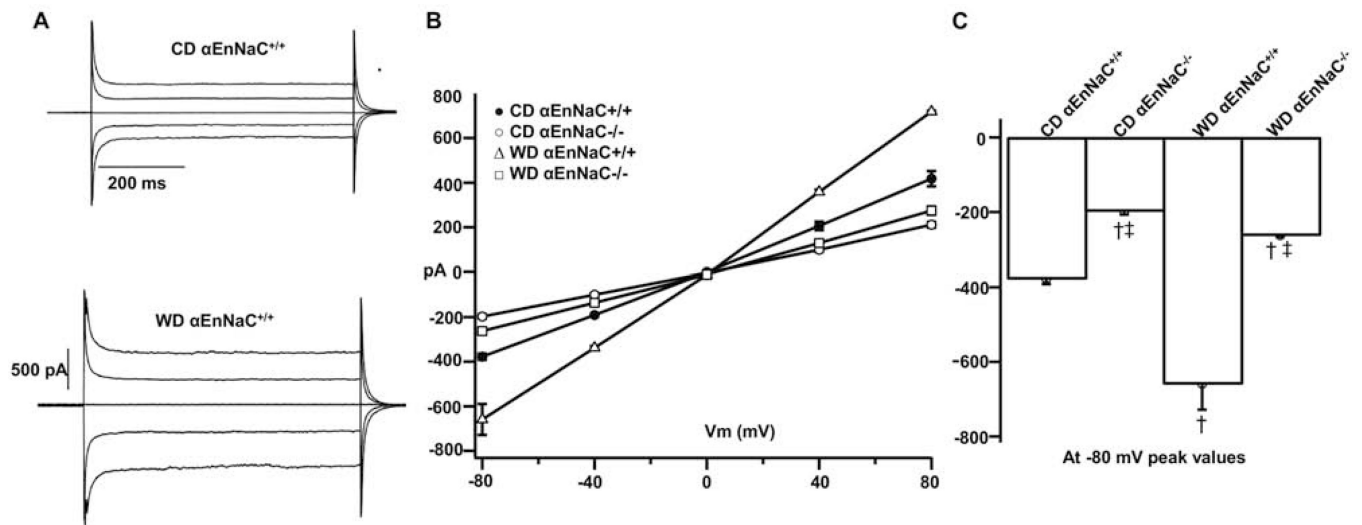


Fig 1. α EnNaC $^{-/-}$ mice prevents WD-induced increases of inward Na^+ currents on isolated lung ECs. Na^+ current tracings (A), group I-V curves of Na^+ currents (B), and comparison of peak inward Na^+ currents at -80 mV (C) in α EnNaC $^{+/+}$ and α EnNaC $^{-/-}$ mice fed a WD, $n=31-38$ cells. † $p < 0.01$ compared with CD α EnNaC $^{+/+}$ group; ‡ $p < 0.01$ compared with CD or WD α EnNaC $^{+/+}$ group in multiple comparison analysis.

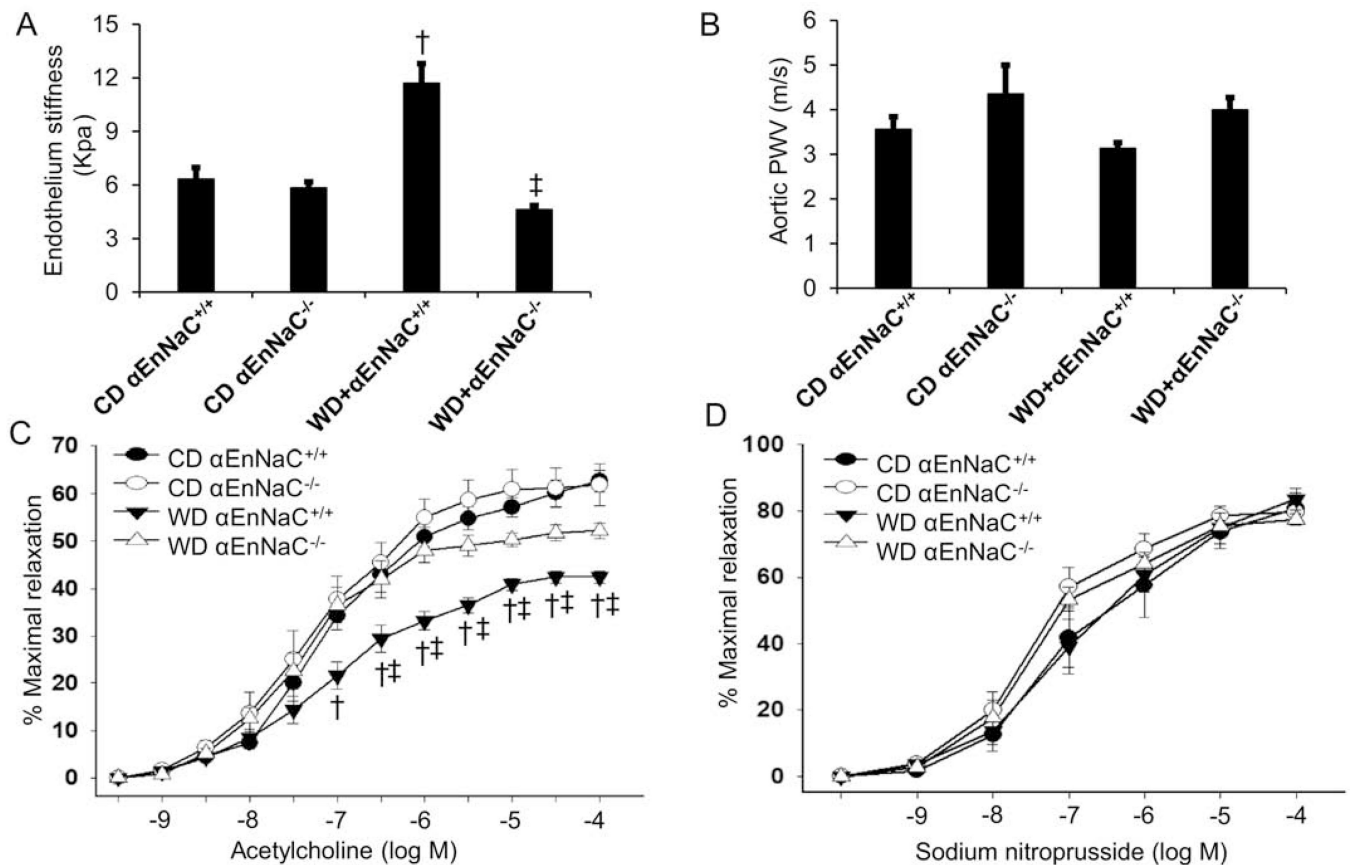


Fig 2. $\alpha\text{EnNaC}^{-/-}$ mice prevents WD-induced endothelium stiffness and impaired aortic relaxation. (A) The *ex vivo* measurement of endothelium stiffness by using atomic force microscopy. n=4–5. (B) Aortic pulse wave velocity measured *in vivo*, n=4–7. (C-D) Vasodilator responses of isolated aortic rings to the endothelium-dependent dilators, acetylcholine (C) and to the endothelium-independent vasodilator, sodium nitroprusside (D). n=5–9. [†] $p < 0.05$ compared with CD $\alpha\text{EnNaC}^{+/+}$ group; [‡] $p < 0.05$ compared with WD $\alpha\text{EnNaC}^{+/+}$ group in multiple comparison analysis.

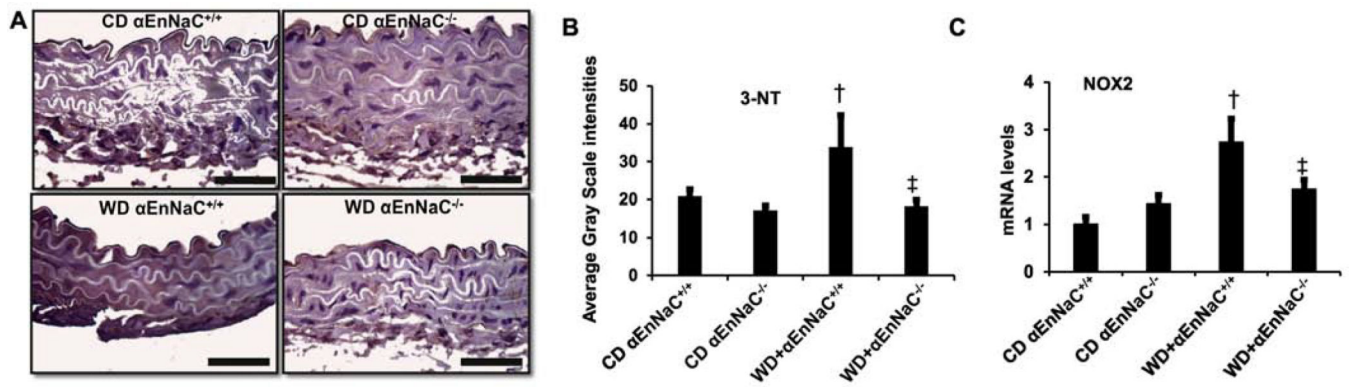


Fig 3. $\alpha\text{EnNaC}^{-/-}$ mice prevents WD-induced aortic oxidative stress. (A) Representative images of aortic sections stained for 3-nitrotyrosine (3-NT), a marker of oxidant stress from accumulation of oxidant peroxynitrite (ONOO^-) with corresponding quantitative analysis (B). Scale bar = 50 μm , $n=5-6$. mRNA levels of Nox2 (C) in aortic tissues as measured by real-time PCR. $n=5-7$. † $p<0.05$ compared with CD $\alpha\text{EnNaC}^{+/+}$ group; ‡ $p<0.05$ compared with WD $\alpha\text{EnNaC}^{+/+}$ group in multiple comparison analysis.

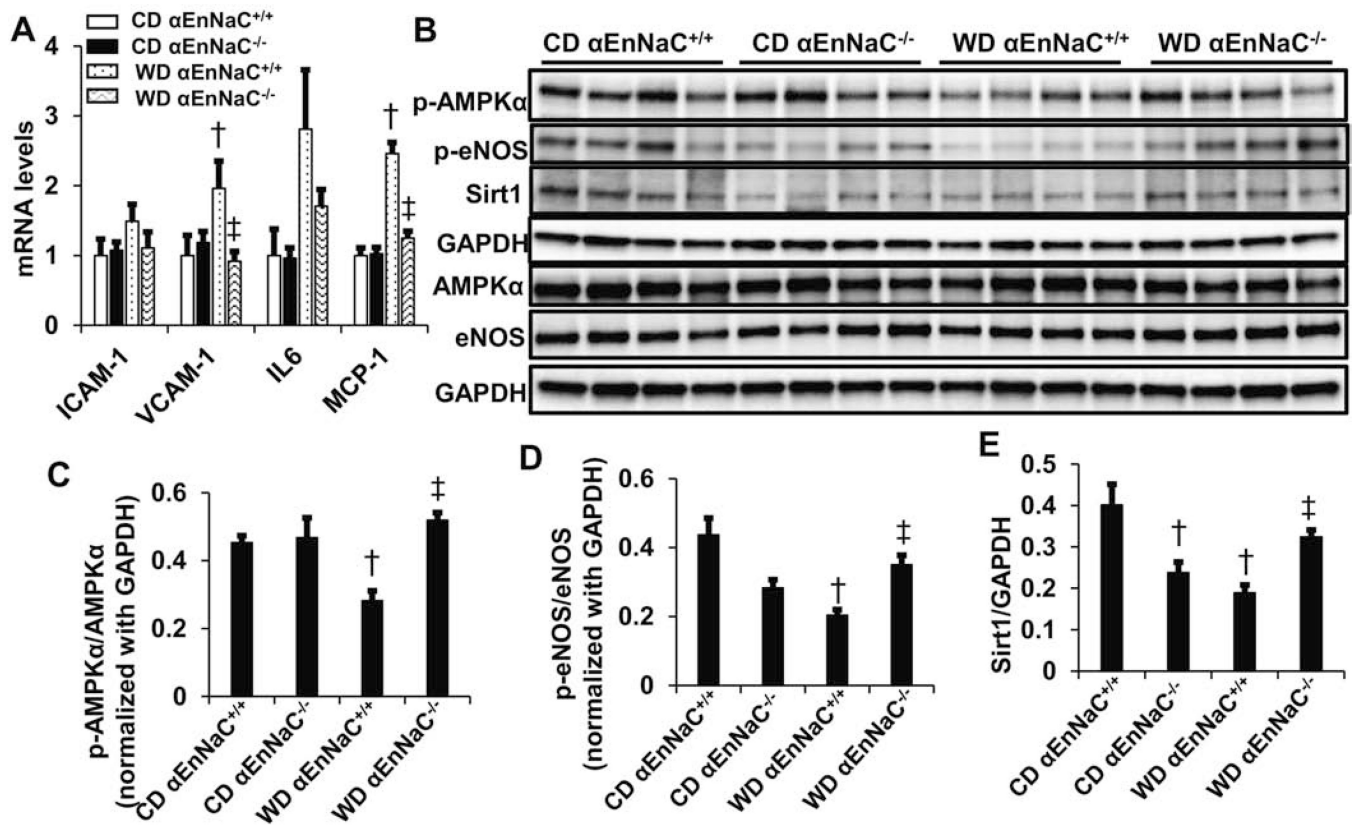


Fig 4.

α EnNaC^{-/-} mice prevents WD-induced an increase of inflammation and reduction of AMPK α and eNOS activity and Sirt1 expression. (A) mRNA levels of ICAM-1, VCAM-1, IL6, MCP-1. (B) The protein abundance of AMPK α , eNOS, Sirt1 and GAPDH in aortic tissues were performed with immunoblotting. Quantitative analysis of protein abundance in p-AMPK α (C), p-eNOS (D), and Sirt1 (E). † $p < 0.05$ compared with CD α EnNaC^{+/+} group; ‡ $p < 0.05$ compared with WD α EnNaC^{+/+} group in multiple comparison analysis.

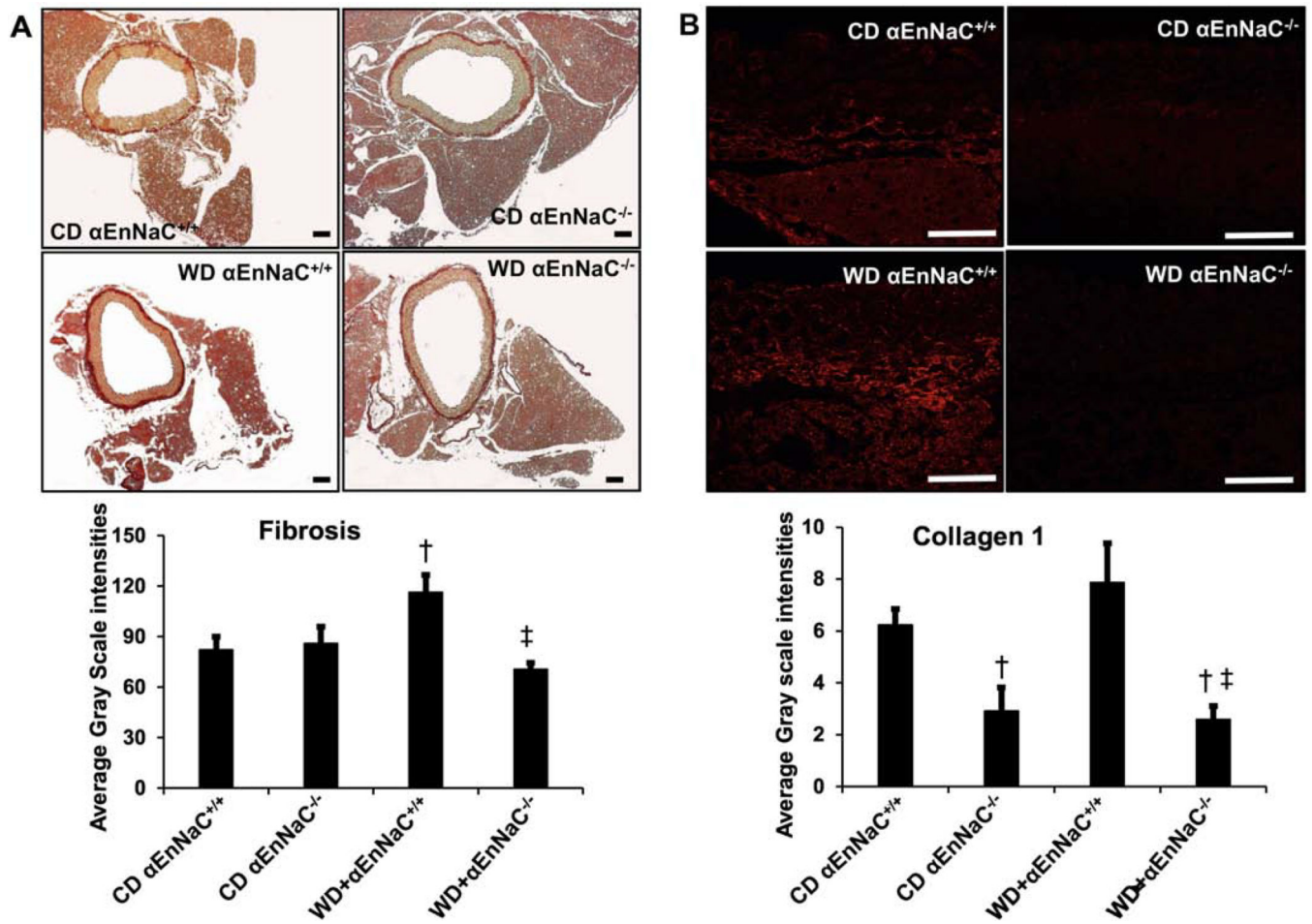


Fig 5. $\alpha\text{EnNaC}^{-/-}$ mice prevents WD-induced aortic remodeling. Representative micrographs show aortic fibrosis staining with picrosirius red staining (A) and collagen 1 (B) with corresponding measures of average gray scale intensities. Scale bar = 50 μm , $n=5-6$. [†] $p<0.05$ compared with CD $\alpha\text{EnNaC}^{+/+}$ group; [‡] $p<0.05$ compared with WD $\alpha\text{EnNaC}^{+/+}$ group in multiple comparison analysis.

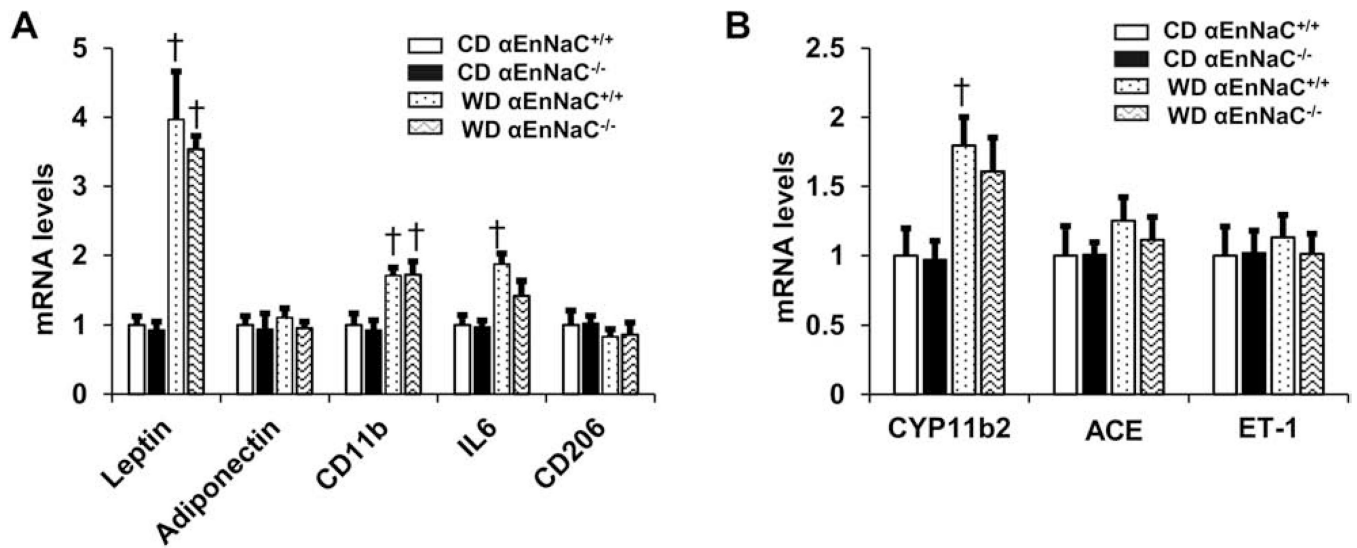


Fig. 6. Deletion of α EnNaC in mice does not prevent WD-induced increases in inflammatory factors and CYP11b2 in abdominal aortic perivascular adipose tissue. (A) mRNA levels of adipokines in leptin, adiponectin, CD11b, IL6 and CD206. (B) mRNA levels of CYP11b2, ACE and ET-1. N=5-7. † $p < 0.05$ compared with CD α EnNaC^{+/+} group in multiple comparison analysis.

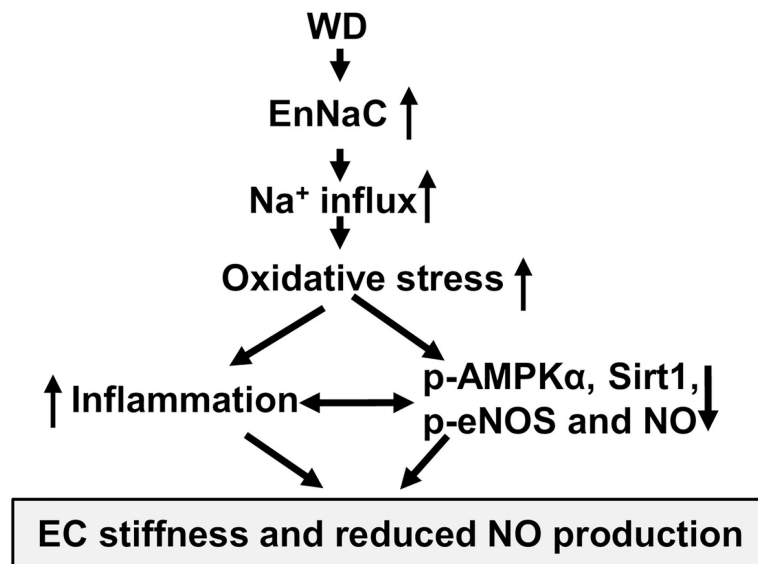


Fig 7. Schematic diagram showing proposed mechanisms underlying the contribution of EnNaC to diet-induced increases in endothelial stiffness and impaired aortic NO mediated vascular relaxation.

Table 1.

Characteristics of mice fed a western diet

Measures	CD α EnNaC ^{+/+}	CD α EnNaC ^{-/-}	WD α EnNaC ^{+/+}	WD α EnNaC ^{-/-}
Fat mass (g)	3.70±0.44	4.04±0.25	7.08±0.70 [†]	6.17 ±0.35 [†]
Lean mass (g)	15.43±0.39	14.99±0.45	14.77±0.30	13.92±0.17
Body weight (g)	20.59±0.63	20.92±0.37	23.59±0.46 [†]	22.17±0.49
Peri-reproductive fat (mg)	651.38±46.56	550.57±40.94	980.72±110.45 [†]	899.04±50.82 [†]
Cholesterol (mg/dl)	80.60±11.37	66.71±4.88	101.83±10.35	100.11±4.50
Triglycerides (mg/dl)	39±2.94	31.71±3.39	42.67±2.67	41.44±5.29
Retro-peritoneal fat (mg)	125.78±25.27	94.44±9.91	181.33±12.99	173.89±11.89
Fasting glucose (mg/dL)	130.8±7.3	153.4±7.3	179.2±31.9	175.9±10.0
HOMA-IR (Arbitrary units)	2.78±0.51	2.90±0.19	3.21±0.46	3.23±0.47
Systolic BP (mmHg)	109.1±4.9	109.4±4.0	106.1±3.2	99.1±1.6
Diastolic BP (mmHg)	56.7±4.7	61.3±3.8	63.1±3.6	56.4±1.2
Pulse pressure (mmHg)	52.4±3.5	48.1±0.7	43.1±3.4	42.6±2.1

Values are mean ± SE. n=5-8.

[†]P<0.05 vs CD EnNaC^{+/+}.

Author Manuscript

Author Manuscript

Author Manuscript

Author Manuscript